

M2 Proton Channel Structural Validation from Full-Length Protein Samples in Synthetic Bilayers and *E. coli* Membranes**

Yimin Miao, Huajun Qin, Riqiang Fu, Mukesh Sharma, Thach V. Can, Ivan Hung, Sorin Luca, Peter L. Gor'kov, William W. Brey, and Timothy A. Cross*

Membrane protein structure and function, especially for small membrane proteins, can be highly sensitive to the membrane mimetic environment used for structural characterization, as exemplified by the M2 protein from influenza A virus that has been characterized in liquid crystalline lipid bilayers, detergent micelles and in detergent-based crystals.^[3–8] Various transmembrane (TM) helical tilt angles, different drug binding sites and amphipathic helix interactions, as well as a lack of consensus on the sidechain geometry for the functionally critical residues is apparent from this set of structures. Many of these structural differences can be explained based on the influence of the protein's environment. Hydrophobic thickness influences the helical tilt; detergent penetration into the helical bundle and crystal contacts influence the packing and hence tilt of the helices, while the highly curved surface of micelles destabilize the interactions of amphipathic helices with what would be the bilayer interface.^[9] These structural perturbations can influence functional properties such as the binding of the antiviral drug to the protein and our understanding of the proton channel functional mechanism. Exactly how well the native membrane needs to be modeled to achieve a native membrane protein structure is explored here, where we aim to validate the structure of the tetrameric M2 conductance domain (M2CD; residues 22–62; PDB #2L0J) that has been structurally characterized in synthetic lipid bilayers. We have set out to do this by observing the full-length protein in synthetic bilayers, as well as in native *E. coli* membranes. For the first time we report on structural insights from the full-length M2 (M2FL) protein using magic angle spinning solid state NMR (ssNMR) and we present spectra of

the protein as it is inserted into the *E. coli* membranes by the cellular apparatus without ever being exposed to a detergent environment. These results validate the earlier structural results obtained from the M2CD observed in a liquid crystalline bilayer environment.

In addition to its proton channel activity, M2 facilitates viral budding that localizes the protein to this site on the surface of an infected cell suggesting that M2 is not imbedded in the high cholesterol and sphingomyelin environment that dominates the viral particle.^[10,11] Instead, M2 appears to be preferentially localized to the periphery of the raft-like lipid domains from which the viral particle buds and where the amphipathic helices of the M2 protein can induce membrane curvature. For this reason and because it has recently been shown that raft-like lipids do not support an M2 conformation compatible with amantadine (the antiviral drug that targets M2) binding^[12] nor do these lipids support a conformation having pK_a values for the His37 tetramer (the critical residues for proton transit) consistent with high proton affinity,^[13] consequently, we have used liquid crystalline lipid environments for M2 that support both of these functional properties.^[14] The synthetic lipid bilayer we have used is the same as that used for the structural study of M2CD,^[7] and the second is another liquid crystalline domain, that of the *E. coli* plasma membrane, an environment that models the lipid and protein complexity of the environment surrounding raft-like domains. Previously, several solid state NMR in situ studies of other membrane proteins in cellular membranes have been reported.^[15–20] Here, we use an in situ preparation to validate a structure of a proven drug target for influenza A. Such validation is necessitated by the sensitivity of this protein's structure to its membrane mimetic environment used for structural studies.

The M2 proton channel is a tetramer of a 97 residue protein having a single (TM) helix^[21] including the H₃₇-xxxW₄₁ signature sequence for a proton channel.^[22] The functional mechanism involves shuttling protons across the central energy barrier facilitated by these four His₃₇ residues, while the Val₂₇ and Trp₄₁ tetramers act as gates at the entrance and exit of the pore, respectively.^[6,7,23–26] ¹³C-¹³C correlation spectra of uniformly [¹³C,¹⁵N]-valine-labeled M2FL (Figure 1 A, B, E) and uniformly [¹³C,¹⁵N]-alanine-labeled M2FL (Figure 1 C, D, F) in reconstituted liposomes and in *E. coli* membranes are very similar in these two environments. The liposome samples represent protein that has been isolated and purified using detergents and then reconstituted into lipid bilayers (Supporting Information). The in situ samples were prepared by simply isolating the *E. coli* cellular membranes

[*] Y. Miao, H. Qin, Dr. R. Fu, Dr. M. Sharma,^[#] T. V. Can,^[§] Dr. I. Hung, Dr. S. Luca,^[†] P. L. Gor'kov, Dr. W. W. Brey, Dr. T. A. Cross
Department of Chemistry and Biochemistry, Institute of Molecular Biophysics, National High Magnetic Field Lab
Florida State University, Tallahassee, FL 32306 (USA)
E-mail: cross@magnet.fsu.edu

[†] Present address: Department of Pharmaceutical Sciences, University of Nebraska, Medical Center, Omaha, NE 68198-6025 (USA)

[§] Present address: Department of Chemistry, Massachusetts Institute of Technology, Cambridge, MA 02139 (USA)

[#] Present address: Department of Biological Chemistry & Molecular Pharmacology, Harvard Medical School, Boston, MA 02115 (USA)

[**] This work was supported by the National Institutes of Health Grants AI23007 and AI074805. Some of the research was conducted at the National High Magnetic Field Laboratory supported by Cooperative Agreement 0654118 between the Division of Materials Research of the National Science Foundation and the State of Florida.



Supporting information for this article is available on the WWW under <http://dx.doi.org/10.1002/anie.201204666>.

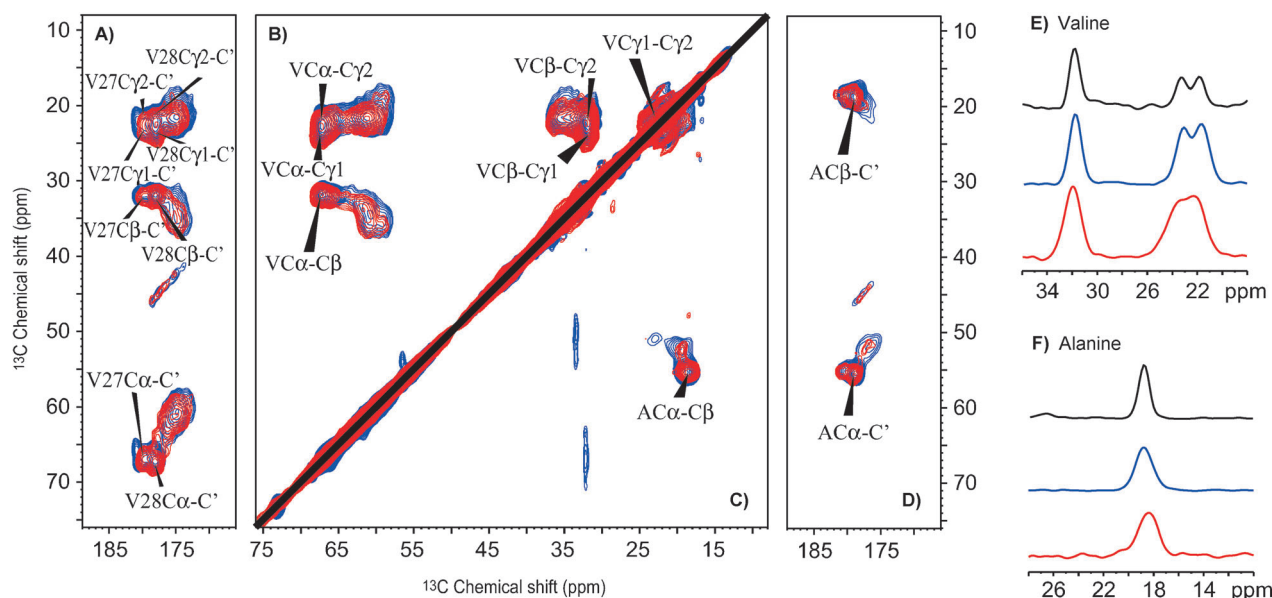


Figure 1. Comparison of ^{13}C - ^{13}C correlation spectra using 50 ms mixing time at 243 K of uniformly [^{13}C , ^{15}N]-valine-labeled M2FL (A, B, E) and uniformly [^{13}C , ^{15}N]-alanine-labeled M2FL (C, D, F) in reconstituted liposomes at pH 7.5 (blue) and in *E. coli* membranes at pH 8.0 (red). A, D) $\text{C}\alpha$, $\text{C}\beta$, $\text{C}\gamma_1$, and $\text{C}\gamma_2$ correlations with C' for valine and $\text{C}\alpha$, $\text{C}\beta$ correlations with C' for alanine-labeled samples. B, C) Correlations between $\text{C}\alpha$, $\text{C}\beta$, $\text{C}\gamma_1$, and $\text{C}\gamma_2$ for valine and $\text{C}\alpha$ - $\text{C}\beta$ correlations for alanine-labeled samples. E) Spectral slices at $\delta = 67.3$ ppm through the valine resonances from M2CD (black), M2FL reconstituted (blue), and M2FL in situ samples (red). F) Spectral slices at 55.5 ppm through the alanine resonances from M2CD (black), M2FL reconstituted (blue), and M2FL in situ samples (red).

from an isotopically labeled culture expressing M2FL (Supporting Information).

There are seven valine and five alanine residues in M2FL: Val₋₁₄ and Ala₋₁ in the N-terminal purification tag, Val₇ in the N-terminal domain on the viral exterior, Val_{27,28} and Ala_{29,30} in the TM helix, and Val_{68,84,92} and Ala_{83,86} in the C-terminal domain on the viral interior. While there is a lack of resolved resonances, there is excellent secondary structure spectral dispersion especially for the C' , $\text{C}\alpha$, and $\text{C}\beta$ sites of alanine and valine, but also significant spectral dispersion for the $\text{C}\gamma_1$ and $\text{C}\gamma_2$ resonances of valine. The conformation-dependent frequencies span characteristic frequencies for helix, coil and sheet motifs. The resonance frequencies observed for the M2CD, Val_{27,28} and Ala_{29,30} are indicated on the spectra and in Table S1 (Supporting Information).^[27]

In Figure 1E slices through both full-length spectra and the spectrum of uniformly [^{15}N , ^{13}C]-labeled M2CD at the $\text{C}\alpha$ frequency for the Val₂₇ and Val₂₈ residues in the TM helix are presented. In Figure 1F similar slices through the alanine spectra and the M2CD spectrum at the $\text{C}\alpha$ frequency for the Ala₂₉ and Ala₃₀ residues in the TM helix are presented. The spectral slices show that the resonance frequencies are nearly identical across all three samples for these sites in the TM helix suggesting that the proton conducting pore has the same or nearly the same structure in all three of these samples. However, the resonance linewidths are somewhat broader for the full-length protein samples, especially for the in situ sample even for the TM helix resonances. Outside of the TM helix the resonances as seen in the 2D spectra in both M2FL preparations are substantially broader and hence the resonances are less intense. However, there is a remarkable overlap of the spectral intensity for all of the valine and

alanine spectral intensity from these samples suggesting that the similarity in structure may extend beyond the TM helices to the rest of the protein.

^{13}C - ^{13}C correlation spectra of uniformly [^{13}C , ^{15}N]-labeled M2CD (Figure 2 A,E) and M2FL (Figure 2 C,D) both reconstituted in the same liposome environment as well as uniformly [^{13}C , ^{15}N]-labeled M2 (Figure 2B) in situ show numerous similarities. In the aliphatic-aliphatic regions of M2FL there are broad resonances underlying the narrower resonances. These latter resonances are mostly consistent with the resonances from M2CD, but the former very broad resonances, as seen in Figure 1, are from those regions outside of the conductance domain and hence not present in the spectrum of M2CD. Also as stated previously the resonances of the TM helix appear to be somewhat broader in the M2FL protein than in the M2CD spectra. Even for M2CD the resonance patterns for each of the amino acid types—valine, alanine, leucine, and isoleucine overlap severely making sequence-specific assignments very challenging. Furthermore, even if sequence-specific assignments were achieved, assigning cross peaks between the aliphatic resonances to specific distances without some form of a limited labeling strategy would be very difficult. Here, we focus on the comparison of isotropic chemical shift frequencies for the more unique residues in the TM helix (Pro₂₅, Ser₃₁, Gly₃₄, His₃₇, Trp₄₁, Asp₄₄, and Arg₄₅). To this end we have shown in Figure 2 the aliphatic-aromatic regions of the M2CD (Figure 2E) and M2FL (Figure 2D) samples in reconstituted liposomes. The resonances of the unique residues as well as those for Val_{27,28} and Ala_{29,30} have been uniquely assigned for M2CD.^[27] Most of these resonances can also be readily recognized in the M2FL spectra by their resonance pattern and nearly identical

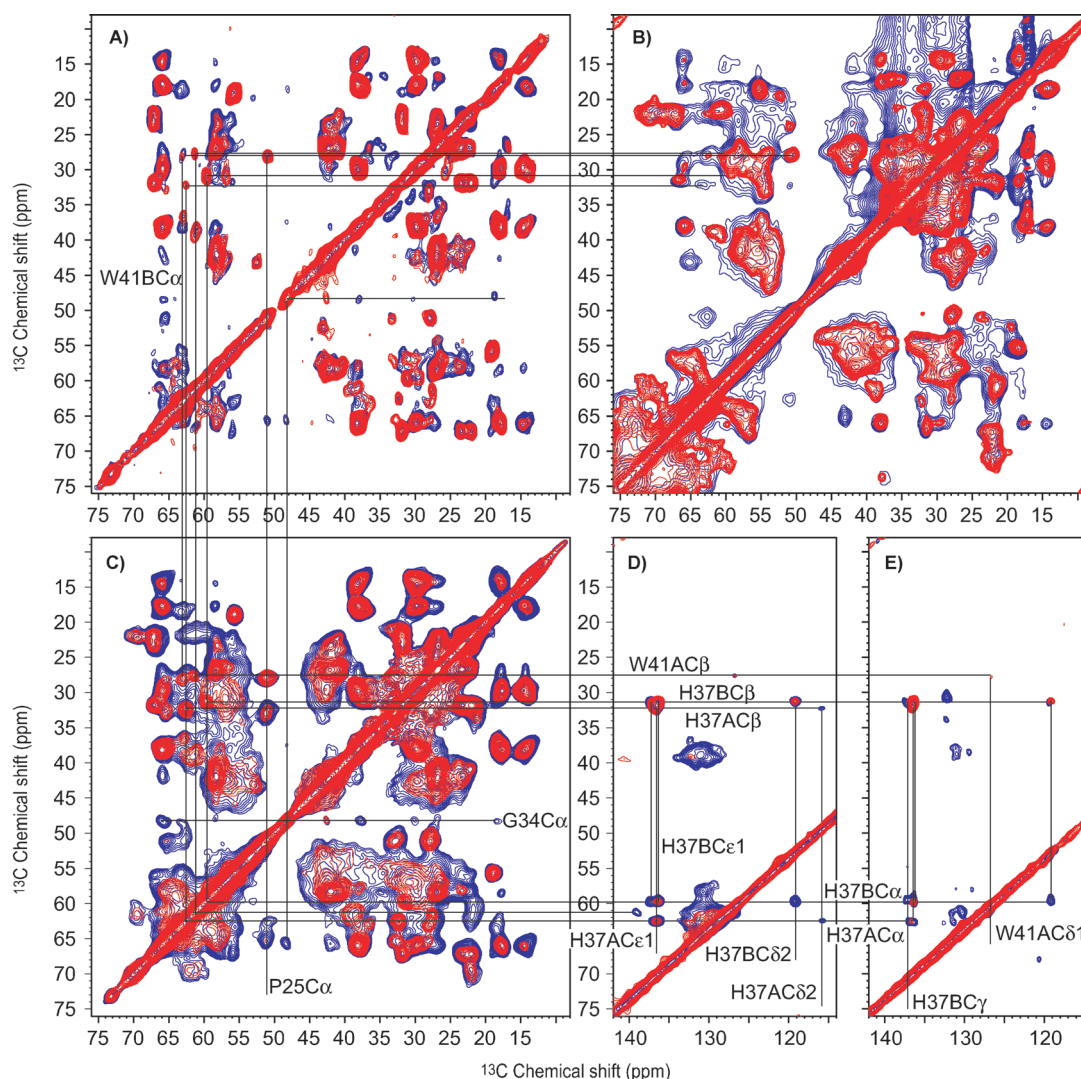


Figure 2. ^{13}C - ^{13}C correlation spectra of uniformly [^{15}N , ^{13}C]-labeled M2CD (A, E) and M2FL (C, D) both in reconstituted liposomes, and M2FL (B) in situ. A–C) Aliphatic–aliphatic regions displaying spectra obtained with 10 (red) and 50 (blue) ms mixing times. D, E) Aliphatic–aromatic regions displaying spectra obtained with 20 (red) and 50 (blue) ms mixing times. Lines drawn between resonances identify similar chemical shifts in the various spectra for which the sequence-specific assignments have been previously achieved for M2CD. All spectra were obtained with ^{13}C -optimized $^1\text{H}/^{13}\text{C}/^{15}\text{N}$ 3.2 mm NMFBL biosolids MAS probe utilizing Low-E coil technology.^[1,2]

frequencies (RMSD for 45 resonances is $\delta = 0.2$ ppm) and the resonance frequencies are given in Table S1.

The M2FL sample reconstituted in liposomes at pH 6.6 exhibits a clear doubling of the His₃₇ and Trp₄₁ C α –C β crosspeaks (Figure 2C) similar to that for M2CD at pH 7.5 (Figure 2A).^[27,28] Such doubling reflects the +2 charged state for the histidine tetrad that has two pK_a values of 8.2 forming imidazole–imidazolium (HisA–HisB) dimers.^[14] The M2FL in situ sample at pH 8.0 does not display so clearly the doubling of the His₃₇ and Trp₄₁ C α –C β crosspeaks, probably due to the high pH of this sample (pH 8.0) and that it is in the midst of the titration for these two pK_a values. As shown in Figure S1 the spectrum of the M2FL reconstituted in liposomes displays a very similar resonance pattern at high pH.

Surprisingly, these histidines near the middle of the lipid bilayer have an affinity for protons that is nearly two orders of magnitude greater than histidines exposed to a polar aqueous

environment. In addition, these charges are close together and would be expected to destabilize the tetrameric structure by charge repulsion. Instead, the formation of two interhelical hydrogen bonds (N ϵ 2–H–N δ 1) between pairs of His₃₇ residues distributes the charge reducing the charge repulsion while stabilizing the tetrameric structure (Figure 3). Indeed, these hydrogen bonds appear to account for the three orders of magnitude increase in structural stability observed between pH 9 and 6.5.^[29] The unique chemistry of the histidine tetrad, actually a dimer of dimers in this charged state, is responsible for shuttling protons across a dehydrated zone in the M2 pore. The +2 charged state observed in the M2CD and M2FL reconstituted liposome samples is known as the histidine locked state, an inactive state. This protein is activated at low pH, presumably by the addition of a third proton to the histidine tetrad leading to proton transport once the Trp₄₁ gate opens.^[7] While each of the imidazoles share a charge in

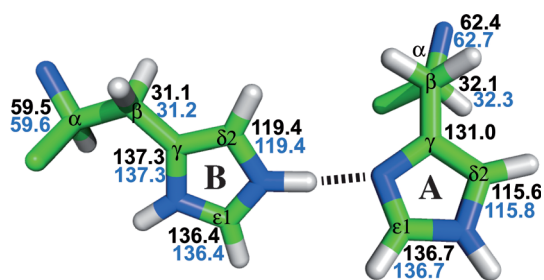


Figure 3. One of the two pair of His37 dimers from the M2CD PDB structure #2L0J, each of which share a charge at pH 6.6 (M2FL sample) and pH 7.5 (M2CD sample). The chemical shifts for these two samples are almost identical: M2FL (blue) and M2CD (black).

the +2 state they do not share the charge equally. A comparison of these resonance frequencies with those of the free amino acid^[30] suggests that the shared protons of the imidazole–imidazolium dimers have a preferred location on the N ϵ 2 site creating more charge density on this imidazole than on its partner that is contributing an N δ 1 site for the hydrogen bond. The histidine residues with the highest charge density have lower C α and C β resonance frequencies and higher C δ 2 resonance frequencies than the pair of histidine residues with lower charge density.

The numerous nearly identical chemical shifts for M2FL and M2CD throughout the TM helix, in particular the structurally and chemically sensitive chemical shifts of the His₃₇ tetrad, suggest that the structure of the M2 pore is essentially identical for the M2CD as for the M2FL protein, thereby validating the conductance domain construct as an appropriate construct for assessing the structure of the M2 proton channel. Furthermore, the uniform overlap of the valine and alanine resonances from M2FL in synthetic lipids and in situ in *E. coli* membranes along with multiple chemical shifts from the TM helix observed in situ in uniformly [¹⁵N,¹³C]-labeled M2FL confirms that the synthetic bilayers represent an adequate environment for supporting a native-like structure. This is particularly significant since the in situ sample has been inserted into the *E. coli* membrane by the cellular apparatus and the protein was observed directly in this environment along with the complex mixture of lipids and native *E. coli* membrane proteins. Therefore, the structure of the M2CD (PDB #2L0J) is validated along with the unique histidine tetrad chemistry responsible for the conductance mechanism.

Received: June 14, 2012
Published online: July 13, 2012

Keywords: M2 protein · membrane proteins · NMR spectroscopy · structural biology · structural validation

- [1] P. L. Gor'kov, E. Y. Chekmenev, C. Li, M. Cotten, J. J. Buffry, N. J. Traaseth, G. Veglia, W. W. Brey, *J. Magn. Reson.* **2007**, *185*, 77.
- [2] S. A. McNeill, P. L. Gor'kov, K. Shetty, W. W. Brey, J. R. Long, *J. Magn. Reson.* **2009**, *197*, 135.
- [3] J. R. Schnell, J. J. Chou, *Nature* **2008**, *451*, 591.
- [4] T. A. Cross, M. Sharma, M. Yi, H. X. Zhou, *Trends Biochem. Sci.* **2011**, *36*, 117.
- [5] R. M. Pielak, J. J. Chou, *Biochem. Biophys. Res. Commun.* **2010**, *401*, 58.
- [6] R. Acharya, V. Carnevale, G. Fiorin, B. G. Levine, A. L. Polishchuk, V. Balannik, I. Samish, R. A. Lamb, L. H. Pinto, W. F. DeGrado, M. L. Klein, *Proc. Natl. Acad. Sci. USA* **2010**, *107*, 15075.
- [7] M. Sharma, M. Yi, H. Dong, H. Qin, E. Peterson, D. D. Busath, H. X. Zhou, T. A. Cross, *Science* **2010**, *330*, 509.
- [8] A. L. Stouffer, R. Acharya, D. Salom, A. S. Levine, L. Di Costanzo, C. S. Soto, V. Tereshko, V. Nanda, S. Stayrook, W. F. DeGrado, *Nature* **2008**, *451*, 596.
- [9] T. A. Cross, H. Dong, M. Sharma, D. D. Busath, H. X. Zhou, *Curr. Opin. Virol.* **2012**, *2*, 128.
- [10] J. S. Rossman, X. Jing, G. P. Leser, R. A. Lamb, *Cell* **2010**, *142*, 902.
- [11] J. S. Rossman, R. A. Lamb, *Virology* **2011**, *411*, 229.
- [12] S. Cady, T. Wang, M. Hong, *J. Am. Chem. Soc.* **2011**, *133*, 11572.
- [13] F. Hu, K. Schmidt-Rohr, M. Hong, *J. Am. Chem. Soc.* **2012**, *134*, 3703.
- [14] J. Hu, R. Fu, K. Nishimura, L. Zhang, H. X. Zhou, D. D. Busath, V. Vijayvergiya, T. A. Cross, *Proc. Natl. Acad. Sci. USA* **2006**, *103*, 6865.
- [15] R. Fu, X. Wang, C. Li, A. N. Miranda, G. J. Pielak, F. Tian, *J. Am. Chem. Soc.* **2011**, *133*, 12370.
- [16] M. Renault, R. Tommassen-van Boxtel, M. P. Bos, J. A. Post, J. Tommassen, M. Baldus, *Proc. Natl. Acad. Sci. USA* **2012**, *109*, 4863.
- [17] T. Jacso, W. T. Franks, H. Rose, U. Fink, J. Broecker, S. Keller, H. Oshkinat, B. Reif, *Angew. Chem.* **2012**, *124*, 447; *Angew. Chem. Int. Ed.* **2012**, *51*, 432.
- [18] A. C. Sivertsen, M. J. Bayro, M. Belenky, R. G. Griffin, J. Herzfeld, *J. Mol. Biol.* **2009**, *387*, 1032.
- [19] B. A. Lewis, G. S. Harbison, J. Herzfeld, R. G. Griffin, *Biochemistry* **1985**, *24*, 4671.
- [20] M. Kamihira, T. Vosegaard, A. J. Mason, S. K. Straus, N. C. Nielsen, A. Watts, *J. Struct. Biol.* **2005**, *149*, 7.
- [21] R. A. Lamb, S. L. Zebedee, C. D. Richardson, *Cell* **1985**, *40*, 627.
- [22] P. Venkataraman, R. A. Lamb, L. H. Pinto, *J. Biol. Chem.* **2005**, *280*, 21463.
- [23] Y. Tang, F. Zaitseva, R. A. Lamb, L. H. Pinto, *J. Biol. Chem.* **2002**, *277*, 39880.
- [24] M. Yi, T. A. Cross, H. X. Zhou, *J. Phys. Chem. B* **2008**, *112*, 7977.
- [25] F. Hu, W. Luo, M. Hong, *Science* **2010**, *330*, 505.
- [26] H. X. Zhou, *Biophys. J.* **2011**, *100*, 912.
- [27] T. V. Can, M. Sharma, I. Hung, P. Gor'kov, W. Brey, T. A. Cross, *J. Am. Chem. Soc.* **2012**, *134*, 9022.
- [28] L. B. Andreas, M. T. Eddy, R. M. Pielak, J. Chou, R. G. Griffin, *J. Am. Chem. Soc.* **2010**, *132*, 10958.
- [29] C. Ma, A. L. Polishchuk, Y. Ohigashi, A. L. Stouffer, A. Schon, E. Magavern, X. Jing, J. D. Lear, E. Freire, R. A. Lamb, W. F. DeGrado, L. H. Pinto, *Proc. Natl. Acad. Sci. USA* **2009**, *106*, 12283.
- [30] S. Li, M. Hong, *J. Am. Chem. Soc.* **2011**, *133*, 1534.